The degenerated glenohumeral joint

histochemical features of matrix degradation and synovial inflammation in patients with omarthrosis and cuff tear arthropathy

From Medical University of Vienna, Vienna, Austria

Cite this article:
Bone Joint Res 2024;13(10):
596–610.

DOI: 10.1302/2046-3758.
1310.BJR-2024-0026.R1

Correspondence should be sent to Stefan Toegel stefan.toegel@muv.ac.at

S. Toegel,[1,2] L. Martelanz,[1] J. Alphonsus,[1] L. Hirtler,[3] R. Gruebl-Barabas,[1] M. Cezanne,[1] M. Rothbauer,[1] P. Heuberer,[4] R. Windhager,[1] L. Pauzenberger[4,5]

[1]Department of Orthopedics and Trauma Surgery, Karl Chiari Lab for Orthopaedic Biology, Medical University of Vienna, Vienna, Austria
[2]Ludwig Boltzmann Institute for Arthritis and Rehabilitation, Vienna, Austria
[3]Division of Anatomy, Center for Anatomy and Cell Biology, Medical University of Vienna, Vienna, Austria
[4]healthPi, Vienna, Austria
[5]Orthopaedic Department, Evangelisches Krankenhaus Wien, Vienna, Austria

Aims

This study aimed to define the histopathology of degenerated humeral head cartilage and synovial inflammation of the glenohumeral joint in patients with omarthrosis (OmA) and cuff tear arthropathy (CTA). Additionally, the potential of immunohistochemical tissue biomarkers in reflecting the degeneration status of humeral head cartilage was evaluated.

Methods

Specimens of the humeral head and synovial tissue from 12 patients with OmA, seven patients with CTA, and four body donors were processed histologically for examination using different histopathological scores. Osteochondral sections were immunohistochemically stained for collagen type I, collagen type II, collagen neoepitope C1,2C, collagen type X, and osteocalcin, prior to semiquantitative analysis. Matrix metalloproteinase (MMP)-1, MMP-3, and MMP-13 levels were analyzed in synovial fluid using enzyme-linked immunosorbent assay (ELISA).

Results

Cartilage degeneration of the humeral head was associated with the histological presentation of: 1) pannus overgrowing the cartilage surface; 2) pores in the subchondral bone plate; and 3) chondrocyte clusters in OmA patients. In contrast, hyperplasia of the synovial lining layer was revealed as a significant indicator of inflammatory processes predominantly in CTA. The abundancy of collagen I, collagen II, and the C1,2C neoepitope correlated significantly with the histopathological degeneration of humeral head cartilage. No evidence for differences in MMP levels between OmA and CTA patients was found.

Conclusion

This study provides a comprehensive histological characterization of humeral cartilage and synovial tissue within the glenohumeral joint, both in normal and diseased states. It highlights synovitis and pannus formation as histopathological hallmarks of OmA and CTA, indicating their roles as drivers of joint inflammation and cartilage degradation, and as targets for therapeutic strategies such as rotator cuff reconstruction and synovectomy.

Article focus

- This study aimed to define the histopathology of degenerated articular cartilage of the humeral head and synovial inflammation of the glenohumeral joint in clinical samples obtained from patients with omarthrosis (OmA) and cuff tear arthropathy (CTA).

Bone & Joint Research

- Another aim was to assess the potential of immunohistochemical tissue biomarkers in reflecting the degeneration status of humeral head cartilage.
- We further tested the hypothesis that histopathological features and immunohistochemical markers allow a discrimination of clinical samples obtained from patients with OmA and CTA, respectively.

Key messages

- Specific histopathological features are associated with cartilage degeneration in OmA and synovial inflammation in CTA when compared to healthy controls.
- Synovitis is a prominent feature of CTA, supporting the association between joint instability and joint inflammation with potential clinical implications regarding surgical interventions and anti-inflammatory therapy.
- The immunohistochemical staining for the C1,2C neoepitope correlated significantly with the histopathological degeneration of humeral head cartilage.
- No difference was found between specimens from patients with OmA and CTA.

Strengths and limitations

- This study provides a comprehensive histological characterization of humeral cartilage and synovial tissue within the glenohumeral joint, both in normal and diseased states.
- It further identified a tissue biomarker that might be useful for future investigations in the context of shoulder pathologies.
- Small sample sizes are a limitation of the study.

Introduction

Osteoarthritis (OA) of the glenohumeral joint (omarthrosis (OmA)) is a degenerative condition known to cause severe pain, limited mobility, and – in severe cases – impairment of arm function. Although OmA is less common than OA of the knee or hip, the shoulder joint ranks among the three most prevalent sites for musculoskeletal pain, following the low back and the knee.[1] With the current understanding that attributes the aetiology of OmA to age-related factors and chronic overuse, it is expected that the rate of upper limb arthroplasty will strongly increase in an ageing population, thus growing into a substantial burden for healthcare systems and societies worldwide.[2]

Total shoulder arthroplasty (TSA) has already become the third most frequently performed joint arthroplasty procedure in the USA,[3] offering pain relief, improved joint function, and an enhanced quality of life. However, there is good reason to explore ways of postponing the necessity for TSA, especially in younger patients or athletes, to minimize the risk of future complications or revision surgeries. Innovative treatment approaches including tissue-engineered scaffolds,[4] stem cell preparations,[5] or stem-cell derived extracellular vesicles[6] might hold promise for regenerating tissue structures or altering the disease process. However, gaining a deeper understanding of the pathogenesis underlying glenohumeral joint degeneration appears crucial for the development and evaluation of targeted therapies, and for determining which patients will benefit the most from various treatment methods. It is important to note that the pathogenesis of OmA is most probably influenced by multiple factors that can be categorized into non-specific and specific factors, as well as systemic and local factors.[7] Traumatic or degenerative rotator cuff tears are a specific risk factor for glenohumeral joint damage,[7] often resulting in degenerative joint changes over time (cuff tear arthropathy (CTA)). Other conditions leading to a degeneration of the glenohumeral joint include shoulder instability,[8] post-traumatic arthritis, rheumatoid arthritis, primary or postoperative infections,[9-11] or surgical procedures.[12]

Prior studies have explored various aspects of the morphological presentation of glenohumeral degeneration, and aimed to elucidate the similarities or potential differences in the pathogenesis of CTA and primary OmA at the tissue level. Early studies using radiological assessment associated idiopathic OmA with articular space narrowing, bony sclerosis, and osteophytosis, and identified a strong association between the changes in OmA and those related to rotator cuff deterioration.[13] The histopathological wear pattern of humeral head cartilage in end-stage OmA (with CTA excluded) was described as central and inferior cartilage damage and loss, thus supporting the macroscopic 'Friar Tuck' pattern, with central eburnation and a surrounding ring of cartilage and osteophytes.[14] In comparison, examination of cadaveric specimens indicated that the presence, but not the size, of a rotator cuff tear resulted in more extensive macroscopic cartilage damage to the glenoid and humeral head than in samples without a tear, and that this damage was predominately situated in the posterior portion of the humeral head.[15] Another histopathological study comparing OmA and CTA specimens found fibrillation, thinning, and tearing of humeral head cartilage in both groups, but thinner remaining cartilage layers in OmA tissues.[16]

Beyond cartilage, synovial inflammation was shown histologically to be increased in CTA patients compared to non-CTA patients,[17] marked by increased immunohistological staining for CD31, CD45, and CD68. Similarly, joint capsule tissue from OmA patients was characterized by increased synovitis, fibrosis, and infiltration by immune cells compared to that from body donors.[18] However, a direct comparison between synovial specimens from OmA and CTA patients still remains absent in the literature.

Building upon this current, albeit somewhat fragmented body of knowledge, this study aimed to define the histopathology of degenerated articular cartilage of the humeral head and synovial inflammation of the glenohumeral joint. In addition, we sought to evaluate the potential of immunohistochemical tissue biomarkers in reflecting the degeneration status of humeral head cartilage. Throughout the study, we were interested in conducting a comparative assessment of clinical specimens obtained from OmA and CTA patients.

Methods

Tissue specimens

A total of 19 patients undergoing anatomical or reverse TSA at the Orthopaedic Department of St. Vincent Hospital, Vienna, Austria were enrolled in this study with written informed consent and in accordance with the terms of the ethics committees of the Medical University of Vienna (EK-No.: 1727/2015) and St. Vincent Hospital Vienna (EK-No.:

201506_EK16). Among these patients, 12 were diagnosed with OmA and seven were diagnosed with CTA. None of the patients had a history of rheumatoid or chronic inflammatory disease. During surgery, a standardized portion of the humeral head including degenerated cartilage, bone, osteophytes, and synovial tissue, as well as a sample of synovial fluid, were collected and transferred under sterile conditions to the Medical University of Vienna. In addition, four glenohumeral joints from three body donors were provided by the Centre of Anatomy and Cell Biology, Medical University of Vienna (EK-No.: 1727/2015).

Histology

Each humeral head was cut into wedge-shaped pieces to provide four section planes: 1) in superior to inferior direction; 2) in anterior to posterior direction; 3) at 45° to the superior/inferior line; and 4) in the peripheral zone of the humeral head (Figure 1). The specimens were fixed in 7.5% neutral-buffered formaldehyde solution and decalcified using Titriplex-Tris-solution (Merck, Germany), then dehydrated and embedded in paraffin according to standard procedures. Paraffin sections (2.5 µm) were stained with haematoxylin and eosin (H&E) for morphological evaluation, or Safranin O (SO) for evaluation of glycosaminoglycan content, and counterstained using light green Goldner III solution.[19] The degree of cartilage degeneration was graded by microscopic evaluation according to the Mankin score (MS) and Osteoarthritis Research Society International (OARSI) score, and the median of the four sections was used for further analysis. The presence or absence of the major histopathological hallmarks of osteoarthritic joint degradation (pannus, reparative fibrocartilage, pore formation, cell clusters (clones), tidemark penetration with blood vessels, eburnation, cavitation (bone cysts), osteophytes) was recorded for each patient/donor. In addition, consecutive sections were stained with Picrosirius red followed by microscopic analysis using polarized light microscopy (PLM) (Zeiss, Germany).[20]

Specimens of synovial tissue were cut to provide three section planes perpendicular to the intima lining layer (Figure 1). Formaldehyde-fixed and paraffin-embedded sections (2.5 µm) were stained with H&E and graded using an established synovitis scoring system.[21] The presence or absence of histopathological hallmarks of synovitis (synovial hyperplasia, stroma activation, inflammatory infiltration) was recorded.

Immunohistochemistry

Based on the above histological evaluation, ten patients (n = 5 OmA and n = 5 CTA) who provided cartilage regions with both mild and severe degeneration were selected. From each patient, one region with MS ≤ 7 and one region with MS ≥ 8 were processed for immunohistochemistry following established protocols.[19,22] The four anatomical humeral heads were included as controls. Immunohistochemical staining using antibodies against collagen type I (#1310-01, Southern Biotech, USA), collagen type II (#1320-01, Southern Biotech), collagen neoepitope C1,2C (#50-1035; IBEX, USA), collagen type X (#58632; Abcam, UK), and osteocalcin (#MAB1419; R&D Systems, USA) was performed using deparaffinized osteochondral tissue sections. Staining was developed using horseradish peroxidase-containing reagent (VECTASTAIN Elite ABC Kit; VectorLabs, USA) and 3,3´-diaminobenzidine tetrahydrochloride hydrate (Honeywell, USA) and H_2O_2 as substrates. Sections were counterstained using Mayer's hemalum solution (Merck, Germany).

For semiquantitative analysis, a Quick Score (QS) index, which is the product of multiplying the labeling index (LI) with staining intensity (SI), was calculated for cartilage specimens.[19] The LI corresponds to the percentage of the immunostained cells (LI = 0: 0% positive cells, 1: 1% to 25%, 2: 26% to 75%, and 3: 76% to 100%). The SI was categorized as follows: SI = 0: negative, 1: weak staining, 2: moderate staining, and 3: strong staining.

Deparaffinized sections of synovial tissue from ten OmA patients were immunohistochemically stained with antibodies against CD3 (#59010; Santa Cruz, USA), CD20 (#70582; Santa Cruz), CD45 (#M0701; Dako, Denmark), and CD68 (#70761; Santa Cruz).

All immunohistological assessments were performed independently by two observers (LM, ST). Cases of deviating assessments were jointly graded to reach agreement.

ELISA

Specimens of synovial fluid from four OmA and four CTA patients were centrifuged at 3,000 × g and 4°C for 25 minutes. Aliquots were snap frozen in liquid nitrogen and stored at -80°C. After thawing, samples were digested using 2 mg/ml hyaluronidase with an effective twofold dilution to improve intra-assay precision.[23] The levels of proMMP-1 (#DMP100), totalMMP-3 (#DMP300), and proMMP-13 (#DM1300) were quantified using commercial enzyme-linked immunosorbent assay (ELISA) kits from R&D Systems.

Statistical analysis

Statistical analyses were performed using SPSS 27.0 (IBM, USA). Categorical data were compared using Fisher's exact test providing p-values and Cramer's V effect sizes (ES ≤ 0.2: weak association; 0.2 < ES ≤ 0.6: moderate; ES > 0.6: strong). Normal distribution of the MS and OARSI score datasets was analyzed using the Shapiro-Wilk test prior to delineation of significances between study groups using analysis of variance (ANOVA) with Tukey post hoc test. For immunohistochemical data, the Mann-Whitney U test was used to compare unpaired groups, whereas the Wilcoxon test was used for comparison of paired groups. For correlation analyses between immunohistochemical parameters and cartilage degeneration (represented by the MS), Spearman's correlation coefficients (r) were calculated and interpreted as follows: 0 to 0.2: weak correlation; > 0.2 to 0.4: mild correlation; > 0.4 to 0.6: moderate correlation; > 0.6 to 0.8: moderately strong correlation; and > 0.8 to 1: strong correlation. ELISA data were analyzed using ANOVA with Tukey post hoc test, and p-values ≤ 0.05 were considered statistically significant with moderate evidence, whereas those < 0.1 were considered to indicate weak evidence or a trend. ELISA data from OmA and CTA patients were compared using the independent-samples *t*-test. In accordance with published guidelines,[24] all analysis units (n) given in figure and table legends refer to the number of independent observations (biological replicates) underlying the respective descriptive statistics and statistical tests.

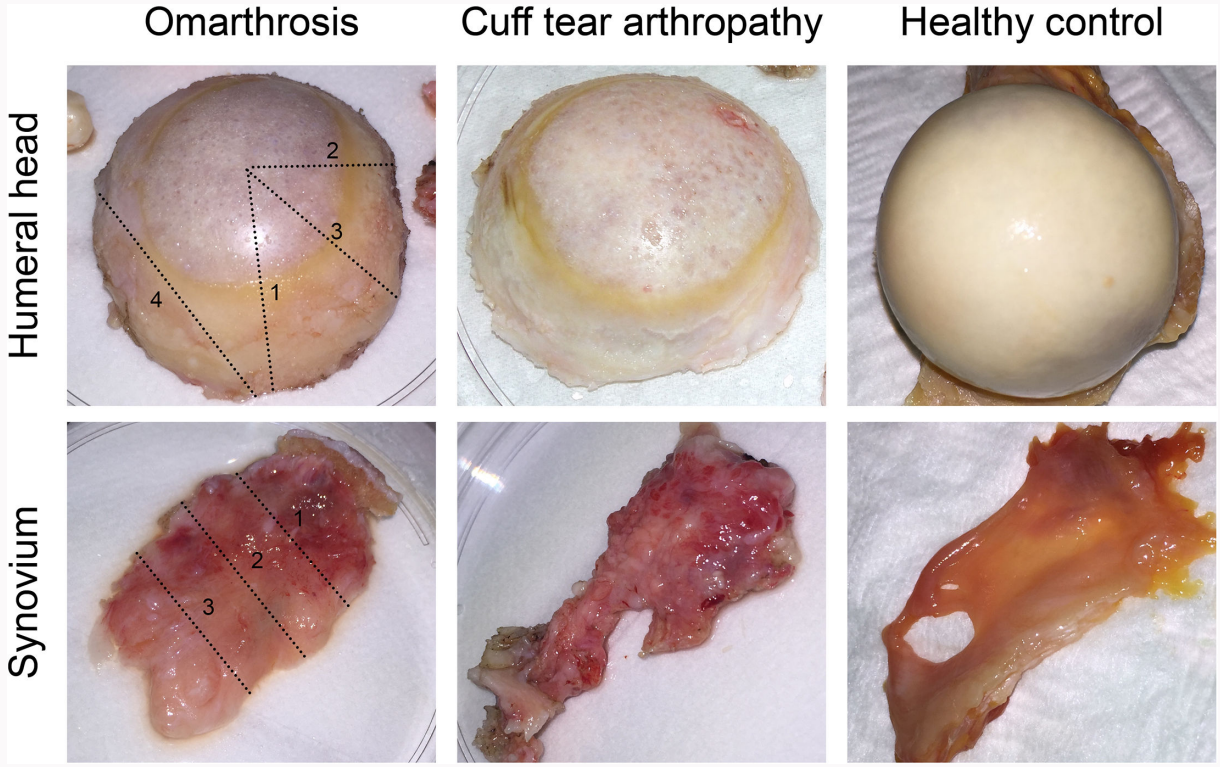

Fig. 1
Macroscopic appearance of clinical specimens. A total of 12 patients with omarthrosis (OmA) and seven patients with cuff tear arthropathy (CTA) were included in the study and compared to four healthy joints from three body donors. Images of representative tissue specimens of the humeral head and the synovium were obtained from OmA, CTA, and controls. The dashed lines indicate the four section plains that were used for histological analysis of each humeral head: 1) superior to inferior direction; 2) anterior to posterior direction; 3) at 45° to the superior/inferior line; and 4) across the peripheral zone of the humeral head. Similarly, three section planes were used across each specimen of synovial tissue.

Results

This study comprises clinical samples of the shoulder joint from OmA patients (mean age 72.8 years (SD 7.0); nine females, three males), CTA patients (mean age 77.0 years (SD 5.7); six females, one male), and body donors (mean age 69.0 years (SD 14.7); one female, three males). There were no differences in the age and sex distribution among the three groups of individuals. Macroscopic examination of the specimens indicated severe degradation of cartilage of the humeral head in OmA and CTA groups. In line with previous reports, we found thinner cartilage thickness and eburnations predominantly in the central region and more preserved cartilage at the periphery (Figure 1). Humeral head cartilage of healthy controls was macroscopically intact. Synovial tissues of OmA and CTA patients presented macroscopic signs of hyperplasia, hypervascularity, and synovitis, whereas for anatomical specimens only minor anomalies were detected (Figure 1).

Proceeding with histological analyses, the tissue degeneration of humeral head cartilage was first graded using the MS and the OARSI score in all study groups. The mean MS were 8.1 (SD 1.0) and 8.0 (SD 1.1) in OmA and CTA patients, respectively, thus being significantly higher than that in the controls (5.3 (SD 2.4); $p < 0.05$, ANOVA with Tukey post hoc test). Results using the OARSI score confirmed these results. Neither score revealed significant differences in cartilage degeneration between OmA and CTA (Table I).

Then, histological sections of the cartilage specimens were examined microscopically for histopathological hallmarks of osteochondral degeneration (Table I, Figure 2). In general, the hallmarks were observed to varying degrees in 50% to 100% of OmA patients, 42% to 100% of CTA patients, and 0% to 50% of controls. Representative histological images are presented in Figure 2.

Pannus cells covering and eroding into cartilage (Figure 2a) were found in nine out of 12 OmA patients and three out of seven CTA patients, but in none of the controls (Table I). Thus, pannus formation was significantly ($p = 0.019$, Fisher's exact test) and strongly ($V = 0.655$) associated with OmA compared to controls. Similarly, our analyses revealed a significant ($p = 0.008$, Fisher's exact test) and strong ($V = 0.745$) association of OmA with pore formation in the subchondral bone plate (Figure 2b), while such pores were absent in controls. In CTA specimens, a trend for an association with pore formation was observed ($p = 0.061$, Fisher's exact test). The formation of cell clusters (Figure 2c) was recorded in all OmA and CTA patients as well as in 50% (2 out of 4) of the control specimens, resulting in a significant and strong association of clusters with OmA ($p = 0.05$, Fisher's exact test, $V = 0.655$). In some OmA and CTA cases, cell clusters were also found in the deep zone of articular cartilage (Figure 2d). A trend for predominant presence of reparative fibrocartilage was observed in OmA patients ($p = 0.077$, Fisher's exact test; Figure 2e), whereas eburnation was associated with CTA specimens with minor evidence ($p = 0.088$, Fisher's exact test; Figure 2f). Blood vessels compromising the tidemark region (Figure 2g) were present in 11 out of 12 OmA specimens, six out of seven CTA specimens, and two out of four controls,

Table I. Evaluation of the histopathological characteristics of humeral cartilage. Clinical specimens obtained from omarthrosis (OmA) patients (n = 12), cuff tear arthropathy (CTA) patients (n = 7), and controls (n = 4) were processed for histological analysis, and the presence or absence of histopathological hallmarks was recorded. Contingency tables were statistically analyzed using Fisher's exact test and Cramer's V. Cartilage degradation was graded using the Mankin score (MS) and Osteoarthritis Research Society International (OARSI) score prior to statistical analysis using analysis of variance (ANOVA) with Tukey post hoc test (*OmA vs control; **CTA vs control; ***OmA vs CTA).

Variable	Histopathological features								Mean Mankin score (SD)	Mean OARSI score (SD)
	Pannus, n	Reparative fibrocartilage, n	Pore formation, n	Cell clusters, n	Tidemark penetration, n	Eburnation, n	Cavitation, n	Osteophytes, n		
OmA	9/12	8/12	10/12	12/12	11/12	7/12	6/12	6/12	8.1 (1.0)	18.5 (3.0)
CTA	3/7	3/7	5/7	7/7	6/7	6/7	3/7	5/7	8.0 (1.1)	15.8 (1.6)
Control	0/4	0/4	0/4	2/4	2/4	1/4	1/4	2/4	5.3 (2.4)	6.4 (4.6)
OmA vs. CTA: Fisher's exact test; Cramer's V	p = 0.326; V = 0.321	p = 0.377; V = 0.233	p = 0.603; V = 0.141	n.d.	p = 1.000; V = 0.094	p = 0.333; V = 0.284	p = 1.000; V = 0.069	p = 0.633; V = 0.209	N/A	N/A
OmA vs. Control: Fisher's exact test; Cramer's V	p = 0.019; V = 0.655	p = 0.077; V = 0.577	p = 0.008; V = 0.745	p = 0.050; V = 0.655	p = 0.138; V = 0.462	p = 0.569; V = 0.289	p = 0.585; V = 0.218	p = 1.000; V = 0.000	N/A	N/A
CTA vs. Control: Fisher's exact test; Cramer's V	p = 0.236; V = 0.463	p = 0.236; V = 0.464	p = 0.061; V = 0.690	p = 0.109; V = 0.624	p = 0.491; V = 0.386	p = 0.088; V = 0.607	p = 1; V = 0.179	p = 0.576; V = 0.214	N/A	N/A
ANOVA Tukey post hoc	N/A	N/A	N/A	N/A	N/A	N/A	N/A	N/A	*p = 0.004; **p = 0.01; ***p = 0.989	*p < 0.001; **p < 0.001; ***p = 0.156

ANOVA, analysis of variance; CTA, cuff tear arthropathy; N/A, not applicable; n.d., not determined; OARSI, Osteoarthritis Research Society International; OmA, omarthrosis.

thus not qualifying as a significant discrimination parameter. Similarly, cavitations/cysts (Figure 2f) and osteophytes (Figure 2h) were found in both patient and control specimens at comparable ratios.

Interestingly, the data brought no evidence of a significant difference between OmA and CTA in terms of the presence of histopathological hallmarks of osteochondral degeneration.

Next, we aimed to test whether major immunohistochemical markers were differentially expressed in the three study groups or as a function of cartilage degeneration. First, osteochondral specimens from five OmA and five CTA patients were selected that exhibited both mildly (MS ≤ 7) and severely degraded (MS ≥ 8) regions. From each control specimen, an intact region without substantial signs of cartilage degeneration was identified for comparison.

Figure 3a indicates that: 1) the MS of the four study groups were significantly higher than those of the control group; and 2) the severely degraded regions exhibited significantly higher MS than the mildly degenerated regions, thus confirming the successful discrimination of tissue regions for further analyses. Figure 4 shows representative sections of intact control cartilage and a severely degraded cartilage region stained with SO (Figure 4a) and Picrosirius red, followed by light microscopy and PLM, respectively (Figure 4b).

Ensuing immunohistochemical analysis revealed the significantly elevated presence of collagen type I in OmA regions with MS ≥ 8 ($p < 0.05$; Figures 3b and 4c). OmA MS ≤ 7 and CTA MS ≥ 8 showed a trend towards increased collagen type I positivity ($p = 0.079$ and $p = 0.081$, respectively; Mann-Whitney U test). Humeral head cartilage of control specimens was characterized by moderate staining for collagen type II (Figures 3c and 4d), resulting in a high collagen type II/collagen type I ratio as expected for intact cartilage (Figures 4c and 4d). Interestingly, positivity for collagen type II significantly increased in severely degraded (MS ≥ 8) regions of OmA and CTA specimens ($p = 0.018$ in both cases), and a similar trend was observed in CTA MS ≤ 7 regions ($p = 0.075$, Mann-Whitney U test). The presence of C1,2C neoepitopes was low in control cartilage (Figure 4e), and significantly increased in each of the four study groups ($p < 0.05$, Mann-Whitney U test; Figures 3d and 4e). There was also a trend for higher median immunohistochemistry scores in MS ≥ 8 regions than in MS ≤ 7 regions ($p = 0.068$ in case of CTA specimens, Wilcoxon test). With a median immunohistochemistry score of 6 (IQR 4.125 to 7.875),

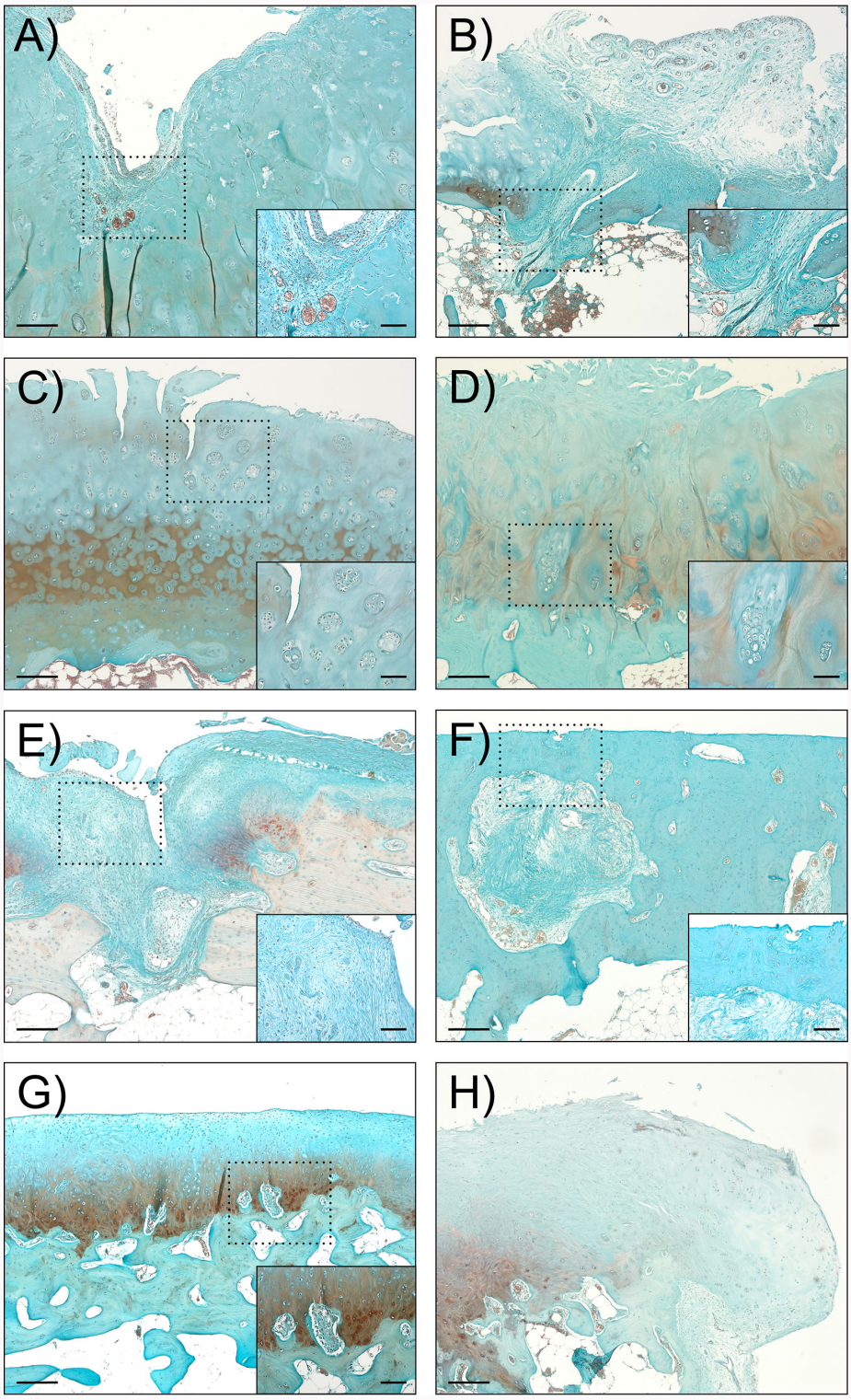

Fig. 2

Representative images of histopathological characteristics observed in humeral cartilage. Clinical specimens of humeral head cartilage were processed for histological staining with Safranin O and observed using light microscopy at 50× (large images) and 400× (inserts) magnification. a) Pannus formation with neovascularization eroding the surface of humeral cartilage. b) Pore formation in the subchondral bone plate. c) and d) Cell clusters in the c) superficial and d) deep zones of cartilage. e) Formation of fibrocartilage-like repair tissue. f) Bony eburnation and subchondral bone cyst. g) Blood vessels penetrating the tidemark. h) Osteophyte formation. Scale bars: 250 µm and 100 µm (inserts).

collagen type X was modestly present in control cartilage (Figure 5c), and showed reduced positivity in patient groups ($p < 0.028$ for MS ≤ 7 CTA, Mann-Whitney U test; Figures 3e and 5c). Staining for osteocalcin showed a heterogeneous pattern among individual patients and did not show differences between the study groups ($p > 0.05$, Mann-Whitney U test and Wilcoxon test; Figures 3f and 5d). None of the assessed immunohistochemical markers showed significant differences between OmA and CTA specimens, neither in mildly nor in severely degraded cartilage regions.

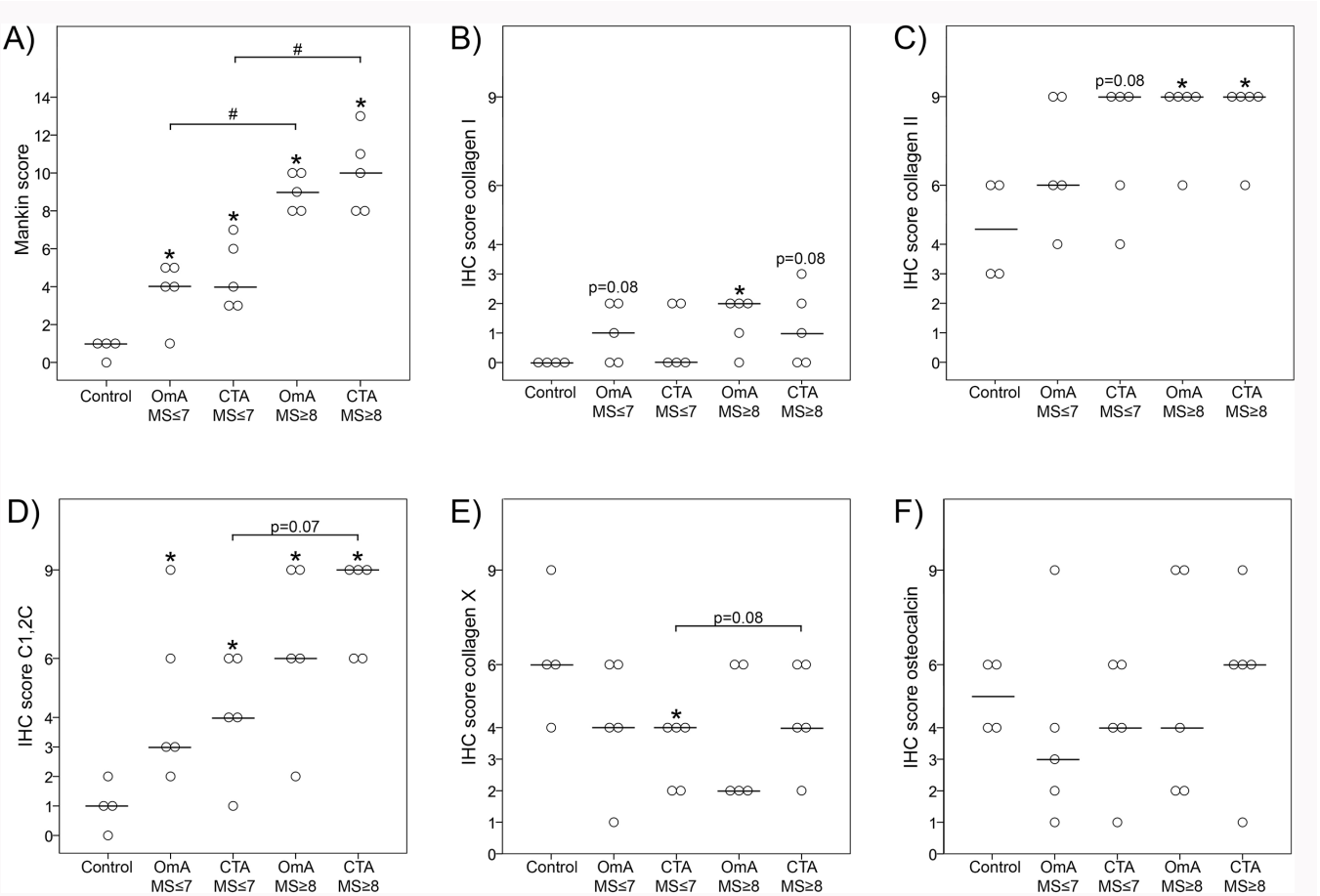

Fig. 3

Immunohistochemical (IHC) scores of degeneration markers in humeral cartilage from omarthrosis (OmA), cuff tear arthropathy (CTA), and controls. Osteochondral specimens from five OmA and five CTA patients were selected that exhibited both mildly (Mankin score (MS) ≤ 7) and severely degraded (MS ≥ 8) regions. Intact cartilage regions were included from control specimens for comparison. All samples were processed for histological staining with a) Safranin O or b) to f) IHC staining with specific antibodies against b) collagen type I, c) collagen type II, d) the C1,2C neoepitope, e) collagen type X, and f) osteocalcin. *p < 0.05 vs control (Mann-Whitney U test for unpaired groups). #p < 0.05: MS < 7 vs MS > 8 (Wilcoxon test for paired groups). p-values between 0.05 and 0.1 are given in exact numbers.

Based on the overall results from Figures 3 to 5, we next hypothesized a correlation between the positivity of humeral cartilage for the immunohistochemical markers and the degree of tissue degeneration. Therefore, we plotted the respective immunohistochemistry scores against the MS of the assessed regions – irrespective of the underlying disease – and found moderate correlation of collagen type I (Figures 6a and 6f), moderate correlation of collagen type II (Figures 6b and 6f), and moderately strong correlation of C1,2C positivity (Figures 6c and 6f) with cartilage degradation. Collagen type X and osteocalcin, in contrast, did not correlate with cartilage degeneration (Figures 6d to 6f).

Synovial tissue of the glenohumeral joint was included from the same patients and donors described above, except that of one CTA patient whose tissue specimen did not meet the criteria of reproducibility in terms of size and integrity. Histological sections were inspected microscopically, and three histopathological parameters (synovial hyperplasia, stroma activation, inflammatory infiltration) were graded using the scoring system of Krenn et al.[21] Representative images of the three parameters in control and OmA specimens are shown in Figure 7a. Overall, the analysis revealed marked synovitis in OmA and CTA patients (median values 4.00 (IQR 2.56 to 5.44) and 3.50 (IQR 2.81 to 4.19), respectively), which was significantly more pronounced in CTA patients compared to control samples (median 2.5 (IQR 1.935 to 3.065); p = 0.020, Mann-Whitney U test) (Figure 7b).

Immunohistochemical analysis of clinical samples affected by synovitis revealed the over-representation of CD68+ macrophages in the synovial lining as well as the presence of CD3+ T cells, CD20+ B cells, and CD45+ leucocytes in the perivascular infiltrates (Figure 8).

A detailed analysis of the histopathological subcategories that sum up to the synovitis score revealed that control samples yielded rather low scores for synovial hyperplasia and inflammatory infiltrates (median 0.25 (IQR -0.19 to 0.69) and 0.25 (IQR 0 to 0.50), respectively) (Figure 7b), whereas stroma activation was found to a more prominent extent (median 1.50 (IQR 1.125 to 1.875); Figure 7b). In OmA and CTA specimens, scores for synovial hyperplasia increased to median 1.00 (IQR 0.31 to 1.69) (p = 0.076; Figure 7b) and 1.00 (0.125; 1.875) (p = 0.022, both Mann-Whitney U test), respectively. Similarly, scores for perivascular infiltrates also increased in OmA and CTA specimens in comparison to controls, albeit without reaching statistical significance (Figure 7b).

Next, we analyzed the synovial fluid of OmA and CTA patients regarding the presence of matrix metalloproteinase (MMP)-1, MMP-3, and MMP-13 levels using ELISA assays. Figure

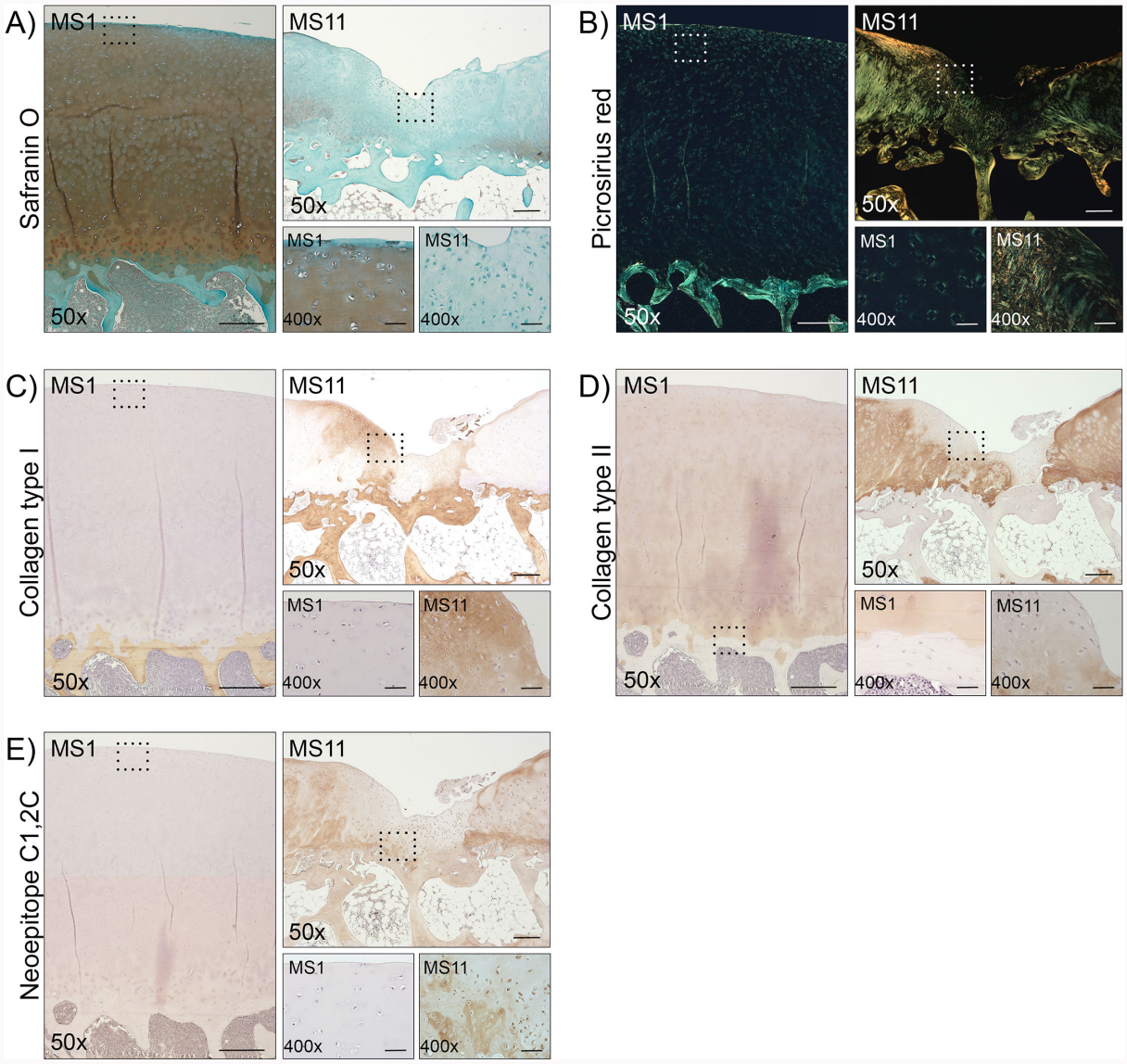

Fig. 4

Presence of matrix-associated markers in the degenerated humeral cartilage. Representative regions of intact (Mankin score (MS) 1) and severely degenerated cartilage (MS11) were selected and stained histologically with a) Safranin O and b) Picrosirius red, or immunohistochemically with specific antibodies against c) collagen type I, d) collagen type II, and e) the collagenase-generated neoepitope C1,2C. Stained sections were observed using light microscopy at 50× and 400× (inserts) magnification. Scale bars: 500 µm (MS1, 50×), 250 µm (MS11, 50×), 50 µm (400×).

9 shows that, irrespective of the underlying disease, MMP-3 levels (mean 222.1 ng/ml (SD 92.9)) were significantly higher than MMP-1 levels (5.8 ng/ml (SD 3.9); $p < 0.001$) and MMP-13 levels (1.9 ng/ml (SD 2.4); $p < 0.001$, ANOVA with Tukey post hoc test). Comparing the data between OmA and CTA patients, we found weak evidence for a difference in case of MMP-1 (mean 16.9 ng/ml (SD 10.5) in OmA vs 5.8 ng/ml (SD 4.0) in CTA; $p = 0.094$, independent-samples *t*-test), and no significant differences in the cases of MMP-3 (mean 383 ng/ml (SD 221) in OmA vs 222 ng/ml (SD 93) in CTA; $p = 0.229$, independent-samples *t*-test) and MMP-13 (median 0.35 ng/ml (IQR -3.82 to 4.52) in OmA vs 1.36 ng/ml (IQR 0.16 to 2.56) in CTA; $p = 1.000$, Mann-Whitney U test).

Discussion

The glenohumeral joint, characterized as a non-weightbearing joint with a relatively thin cartilage layer,[25] distinguishes itself from the weightbearing joints (hip, knee, or ankle joint) primarily due to its unique anatomical and biomechanical features.[26] Furthermore, recent data have suggested the presence of potential metabolic distinctions in the articular cartilage of the shoulder, even when the cartilage maintains normal morphology.[27] While these considerations may imply the existence of specific molecular mechanisms underpinning shoulder joint (patho)physiology, it is worth noting that research focusing on the cellular and tissue-level aspects of the glenohumeral joint still lags behind that of other joints, such as the knee or hip joints.

Histology has probably been the most important structural outcome measure of cartilage degeneration in the context of OA research. It allows for the assessment of the morphology and quality of de- or regenerated cartilage at a resolution that cannot be depicted by MRI or other advanced in vivo imaging techniques. Thus, although

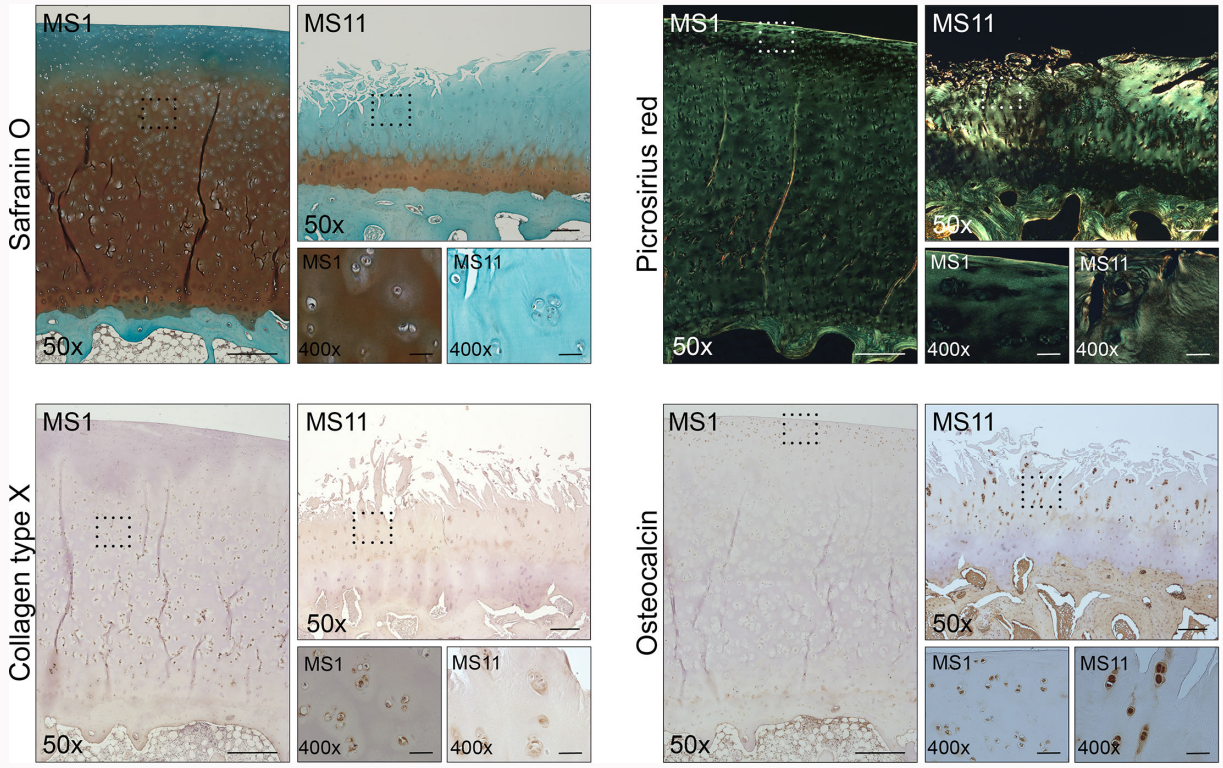

Fig. 5

Presence of chondrocyte hypertrophy-associated markers in the degenerated humeral cartilage. Representative regions of intact (MS1) and severely degenerated cartilage (MS11) were selected and stained histologically with a) Safranin O and b) Picrosirius red, or immunohistochemically with specific antibodies against c) collagen type X or d) osteocalcin. Stained sections were observed using light microscopy at 50× and 400× (inserts) magnification. Scale bars: 500 µm (MS1, 50×), 250 µm (MS11, 50×), 50 µm (400×).

invasive and destructive by nature, histology is still considered the gold standard for biomedical investigations that study joint pathophysiology or aim to develop novel treatment or imaging strategies. In the field of shoulder pathologies, however, a lack of knowledge on the specific histopathological features characterizing glenohumeral joint degeneration potentially impairs our full understanding of the disease, as well as the investigation of novel therapies in relation to structural tissue analysis.

Here, we have shown that cartilage degeneration of the humeral head in OmA patients is associated with the histological presentation of: 1) pannus overgrowing the cartilage surface; 2) pores in the subchondral bone plate; and 3) chondrocyte clusters. Pannus contains proliferating synovial cells that attach to cartilage surfaces and destroy the tissue below, at least partly due to high expression of proteases such as MMPs.[28] The presence of pannus tissue is primarily known from inflammatory arthropathies such as rheumatoid arthritis, including the shoulder, but also occurs in OA of the hip or knee.[28] This study extends these observations by showing that pannus is also present in 'non-inflammatory', degenerative shoulder pathologies, thus contributing to the deterioration of humeral cartilage. On the histological level, our results in the glenohumeral joint largely confirmed the findings of Yuan et al[28] in the knee and hip joint, demonstrating that pannus primarily occurred as foci over the cartilage surface and that it showed moderate cell density with absence of CD68+ cells. Strikingly, 12 out of 19 patients (63%) undergoing total shoulder arthroplasty due to OmA or CTA showed histopathological signs of pannus formation. In a re-evaluation of 13 OA knee joints that were processed and analyzed using the same methodology as in a previous study,[29] we found the presence of pannus tissue in 7/13 patients (54%), which is comparable to the rate in our shoulder samples. This suggests a high rate of pannus formation in the non-rheumatoid glenohumeral joint, even when compared to the rheumatoid hip (71%), knee (90%), or metatarsophalangeal joints (80%).[30]

Under physiological conditions, the subchondral bone plate provides both mechanical and nutritional support for cartilage. Microstructural damage, such as subchondral plate pores that penetrate the calcified cartilage and establish a direct contact between chondrocytes and cells of the bone or the bone marrow, has been discussed to enhance bone-cartilage crosstalk in OA.[31,32] To the best of our knowledge, this report is the first to show the association between subchondral bone pores and humeral cartilage degeneration in OmA and CTA. Under osteoarthritic conditions, the normally quiescent chondrocytes undergo a phenotypic shift characterized by cell proliferation, cluster formation, and increased production of both matrix proteins and matrix-degrading enzymes.[33] These chondrocyte clusters were shown to express increased levels of chondroprogenitor markers,[34] galectins,[35-37] and aberrant nuclear factor kappa B (NF-kB) activation.[38] A recent histopathological study found chondrocyte clusters in the humeral head cartilage of CTA patients, but not in OmA patients.[16] In our study, however, we observed such clusters in all specimens of humeral cartilage of OmA and CTA. Although

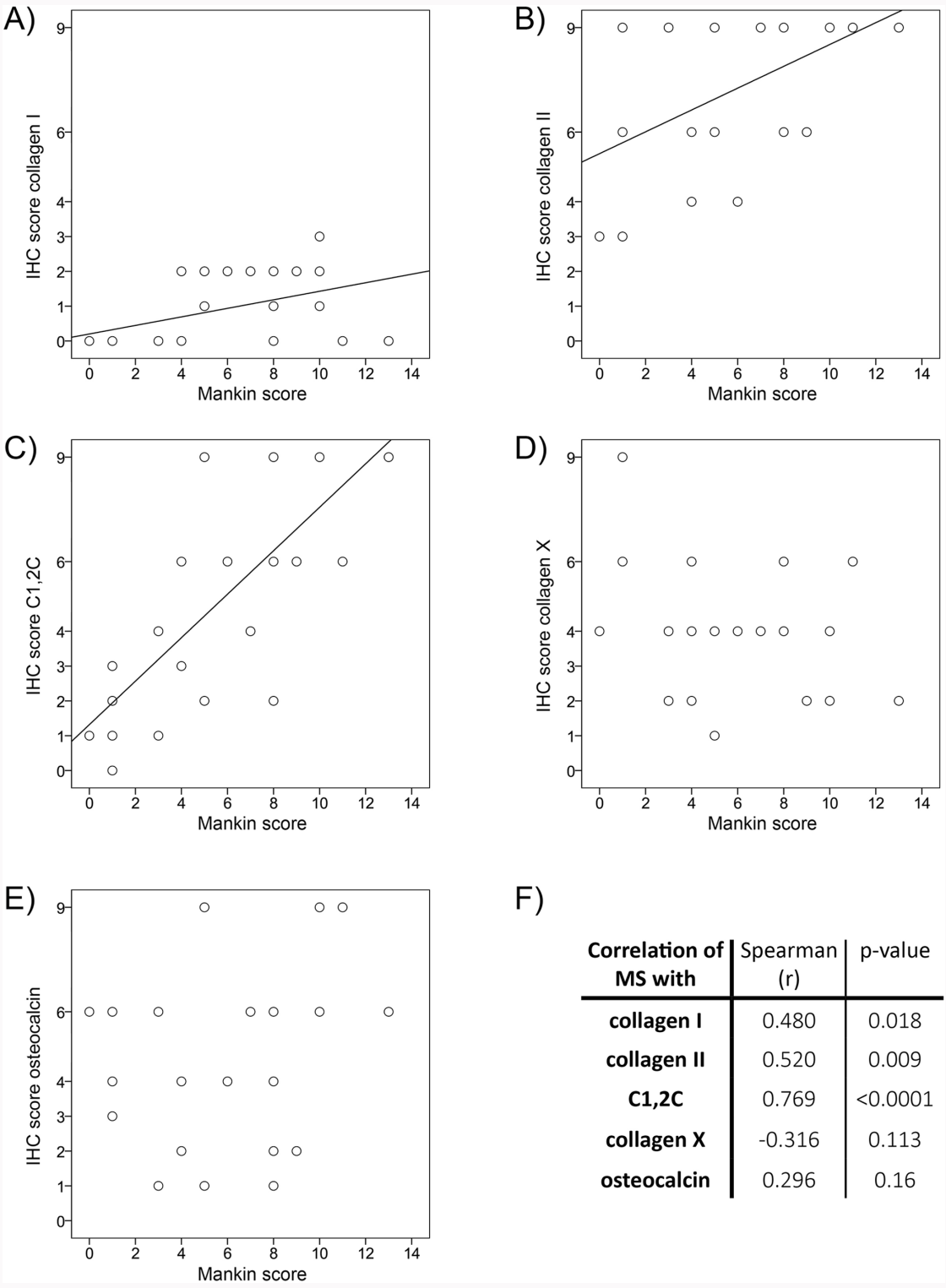

F)

Correlation of MS with	Spearman (r)	p-value
collagen I	0.480	0.018
collagen II	0.520	0.009
C1,2C	0.769	<0.0001
collagen X	-0.316	0.113
osteocalcin	0.296	0.16

Fig. 6

Correlation of immunohistochemical (IHC) markers with the degeneration of humeral cartilage. IHC scores of a) collagen type I, b) collagen type II, c) the C1,2C neoepitope, d) collagen type X, and e) osteocalcin were plotted against the Mankin score (MS) of the respective specimen. Each circle corresponds to one clinical specimen included in this study (n = 12 omarthrosis (OmA) patients, n = 7 cuff tear arthropathy (CTA) patients, and n = 4 controls). f) Spearman correlation coefficients and exact p-values of the data shown in a) to e) are given.

both studies analyzed cartilage specimens obtained at the time of shoulder prosthesis arthroplasty and used comparable histological processing, this conflicting result might stem from the fact that our study analyzed four section planes across the humeral head, whereas the previous study only used one section plane along the middle line on the coronal plane from superior to inferior direction.[16] Furthermore, our study confirms previous reports showing that synovitis accompanies late stages of glenohumeral joint degeneration.[17,18,39,40] A more detailed analysis of histopathological characteristics of the inflammed synovium, however, revealed that the hyperplasia

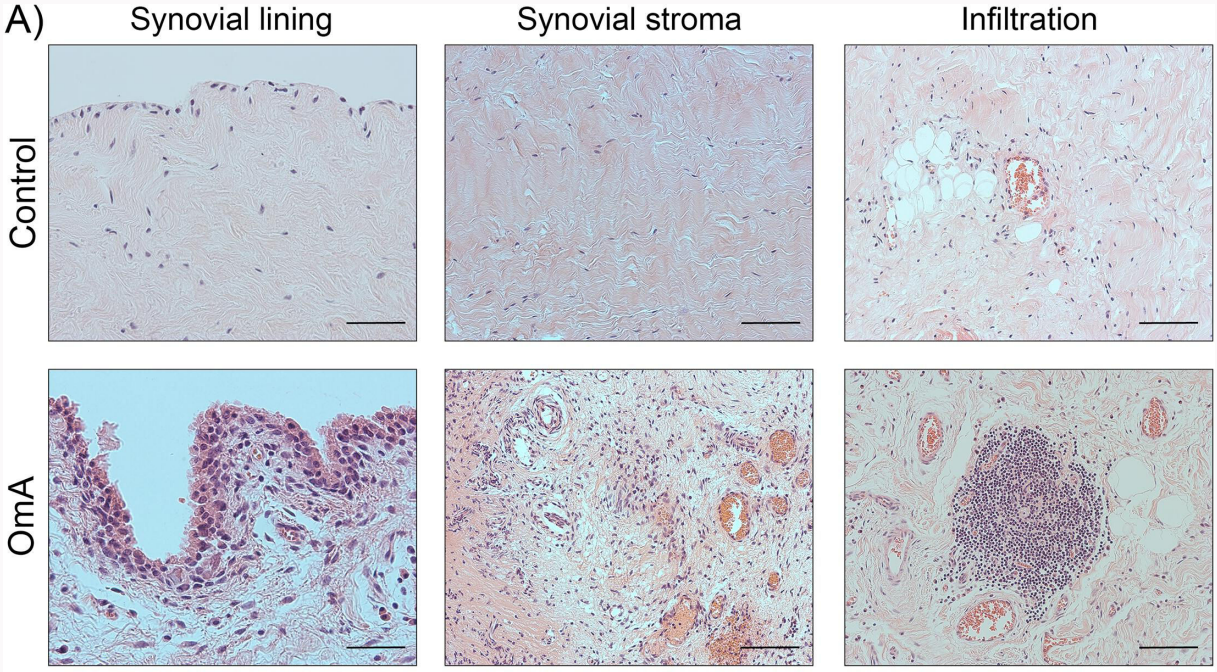

B)

	Synovium			
	Synovial hyperplasia	**Activation of fibroblasts**	**Inflammatory infiltration**	**Synovitis score** (Median±IQR)
OmA	1.00 (0.31; 1.69)	2.00 (0.81; 2.19)	1.00 (0.125; 1.875)	4.00 (2.56; 5.44)
CTA	1.00 (0.875; 1.125)	2.00 (1.875; 2.125)	0.75 (0.25; 1.25)	3.50 (2.81; 4.19)
Control	0.25 (-0.19; 0.69)	1.50 (1.125; 1.875)	0.25 (0; 0.5)	2.50 (1.935; 3.065)
Mann-Whitney-U OmA vs. CTA	p=0.876	p=0.747	p=0.521	p=0.886
Mann-Whitney-U OmA vs. Control	p=0.076	p=0.140	p=0.165	p=0.097
Mann-Whitney-U CTA vs. Control	**p=0.022**	p=0.146	p=0.259	**p=0.020**

Fig. 7

Synovitis scores of omarthrosis (OmA), cuff tear arthropathy (CTA), and control tissues. a) Representative images of the synovial lining, the synovial stroma, and inflammatory infiltrations in control and OmA tissues. The control case represents the absence of synovitis with a normal synovial lining cell layer (one to two cell layers thick), normal cell distribution in the stroma, and slight infiltrations (diffusely distributed and aggregated immune cells). The sum of parameters is 1 out of 9, inflammatory grade = 1. The OmA case represents strong synovitis with strong enlargement of the synovial lining layer (more than five cell layers thick), moderate stroma activation, and moderate inflammatory infiltration (medium-sized lymphatic follicles without germinal centre). The sum of parameters is 7 out of 9, inflammatory grade = 3. Scale bars: 50 µm. b) Semiquantitative evaluation of the three histopathological parameters and total synovitis in OmA (n = 12), CTA (n = 6), and controls (n = 4) was performed using the Krenn score. Presented are the median values with 25th and 75th percentiles in brackets. Statistical analyses were performed using the Mann-Whitney U test. Exact p-values are given, and p-values < 0.05 are displayed in bold font.

of the synovial lining layer is a strong indicator of inflammatory processes in CTA, but only to a lesser extent in OmA.

Taken together, these data provide histological evidence for the concomitant involvement of synovial tissue, subchondral bone, and cartilage in the degenerative processes of the glenohumeral joint. The presence of pannus, subchondral plate pores, chondrocyte clusters, and synovial hyperplasia might be valuable predictors of cartilage breakdown in the glenohumeral joint.

When investigating the extracellular matrix compositions of humeral head cartilage from OmA and CTA patients, the current study observed strong depletion of glycosaminoglycans (as indicated by decreased SO staining) and disorganized arrangement of collagen fibrils (shown using polarization microscopy). For a more detailed analysis, we employed immunohistochemistry to demonstrate that the overall immunopositivity of humeral cartilage for collagen type I and collagen type II significantly correlates with

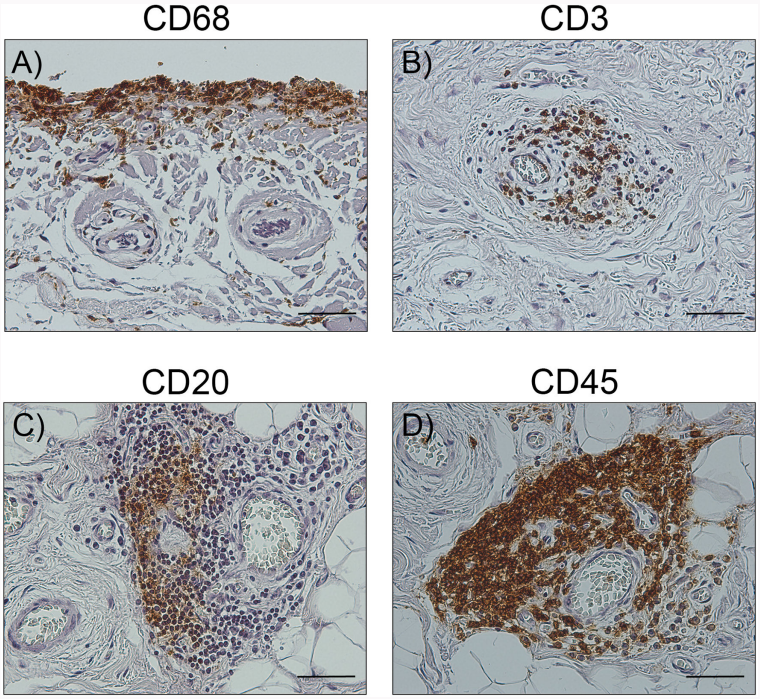

Fig. 8
Immunohistochemical staining of inflammed synovial tissue. Clinical specimens of synovial tissue from a representative omarthrosis (OmA) patient were histologically processed and stained with antibodies against a) CD68, b) CD3, c) CD20, or d) CD45. Immunopositive cells are shown in brown colour. Scale bars: 50 µm.

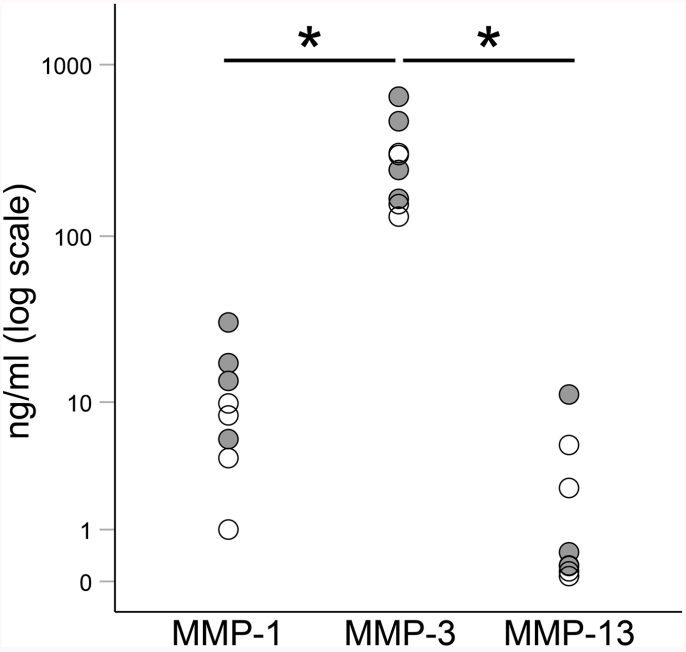

Fig. 9
Levels of matrix metalloproteinases (MMPs) in the synovial fluid of omarthrosis (OmA) and cuff tear arthropathy (CTA) patients. Synovial fluid of OmA (n = 4, grey dots) and CTA (n = 4, white dots) patients were analyzed using enzyme-linked immunosorbent assays (ELISAs) for MMP-1, MMP-3, and MMP-13. Statistically significant differences between the levels of the MMPs are marked with asterisks (*p < 0.05; analysis of variance (ANOVA) with Tukey post hoc test).

cartilage degeneration, corroborating previous data on a significant (13-fold) increase of collagen type 1 messenger RNA (mRNA) levels in OmA compared to non-OmA cartilage.[41] Of note, the increase in positivity for collagen type II is expected to stem from the higher accessibility of epitopes due to the strong depletion of matrix components such as glycosaminoglycans.[42] In focal regions of cartilage lesions, however, we found a substantial shift from collagen type II to collagen type I, reflecting the change of the chondrocyte phenotype under osteoarthritic conditions that has been well

documented in articular chondrocytes from other joints.[33,43,44] The degradation of the extracellular matrix in OmA and CTA cartilage was immunohistochemically demonstrated using an antibody against the C1,2C neoepitope, which is also in line with the marked levels of MMP-1, MMP-3, and MMP-13 that were detected in the synovial fluid of these patients using ELISA. The C1,2C neoepitope was previously used as an immunohistochemical biomarker to assess collagen degradation in human femoral condylar cartilage in situ,[45] in human OA chondrocyte micromass cultures,[46] in organ culture models of the intervertebral disc,[47] or in a murine model of joint surface repair following acute mechanical injury.[48] To our knowledge, the present study provides the first application of the C1,2C neoepitope in the context of shoulder pathologies. It essentially suggests the abundance of this cleavage product as a useful tissue biomarker for glenohumeral cartilage degeneration, which can be a useful outcome parameter in future studies assessing therapeutic interventions.

Prompted by a previous report showing the age-independent association between the histological degeneration grade and cartilage calcification in the shoulder,[49] we sought to evaluate whether immunohistochemical biomarkers of chondrocyte hypertrophy and mineralization (i.e. collagen type X, osteocalcin) could also reflect the degeneration process of humeral OmA cartilage. Interestingly, we found that neither of the two candidates correlated with histopathological degeneration, which might stem from the fact that, in our study, articular chondrocytes were immunopositive for both biomarkers even in intact or mildly degenerated specimens. In contrast, a previous study showed that healthy humeral cartilage from body donors (with a comparable mean age as in our study) were immunonegative for collagen type X.[27] The reason for this discrepancy is currently unknown.

Overall, our investigation of humeral cartilage and synovial tissue found no evidence for a histopathological difference between end-stage OmA and CTA patients in direct comparison. Similarly, protein levels of MMP-1, MMP-3, and MMP-13 were comparable between the two disease patterns. However, it is striking that in comparison to the respective healthy controls, humeral cartilage exhibited significantly elevated histopathological signs in OmA patients (Table I), whereas synovial tissues showed significantly increased features of synovitis in CTA patients (Figure 7b). This finding is in line with the clinical observation that synovitis is among the most common findings during arthroscopic surgery in patients with rotator cuff diseases.[40] Synovial inflammation of the glenohumeral joint correlates with the tear size of the supraspinatus tendon, and is suggested as a source of pain and as a contributor to the pathogenesis of rotator cuff tear.[17,50,51] Idiopathic OmA, in contrast, might be less prone to synovitis than CTA, as also suggested by a comparison of idiopathic OA and post-traumatic arthritis in the knee joints of an animal model.[52] Since natural instability is a hallmark of CTA, increased biomechanical stress might lead to the activation of cellular pathways leading to stimulation of synovial hyperplasia and synovitis.[53] In hindsight of clinical implications, our results support joint stabilization as a reasonable strategy to reduce the progression of osteoarthritic degeneration and synovitis in the glenohumeral joint, as also shown previously in experimental models of other joint diseases.[54,55] Moreover, it has also been shown that synovectomy can reduce chemokines involved in cartilage destruction in OA and rheumatoid arthritis.[56] Consequently, it could be speculated that there is a potential benefit for rotator cuff reconstruction and synovectomy in cases of early-stage CTA to delay progress of degenerative glenohumeral changes. However, this has to be further evaluated in future studies.

In conclusion, this study provides a comprehensive histological characterization of articular humeral cartilage and synovial tissue within the glenohumeral joint, both in normal and diseased states. Of particular interest for future clinical interventions is that our results show the presence of synovitis and pannus formation in shoulder pathologies that are classically regarded as non-inflammatory conditions. We further identified immunohistochemical tissue biomarkers, highlighting the C1,2C neoepitope as an indicator of humeral cartilage degeneration. Of note, however, is that no differences between OmA and CTA were found in the end-stage cases included in this study. Hence, this report establishes a methodological framework for future investigations that aim to assess specific biomarker candidates, uncover the molecular mechanisms of tissue degradation in the glenohumeral joint, examine different OA phenotypes, or explore novel treatment algorithms in the context of shoulder pathologies.

References

1. **Stanborough RO**, **Bestic JM**, **Peterson JJ**. Shoulder osteoarthritis. *Radiol Clin North Am*. 2022;60(4):593–603.
2. **Thomas M**, **Bidwai A**, **Rangan A**, **et al**. Glenohumeral osteoarthritis. *Shoulder Elbow*. 2016;8(3):203–214.
3. **Wagner ER**, **Farley KX**, **Higgins I**, **Wilson JM**, **Daly CA**, **Gottschalk MB**. The incidence of shoulder arthroplasty: rise and future projections compared with hip and knee arthroplasty. *J Shoulder Elbow Surg*. 2020;29(12):2601–2609.
4. **Chainani A**, **Little D**. Current status of tissue-engineered scaffolds for rotator cuff repair. *Tech Orthop*. 2016;31(2):91–97.
5. **Rossi LA**, **Piuzzi NS**, **Shapiro SA**. Glenohumeral osteoarthritis: the role for orthobiologic therapies. *JBJS Rev*. 2020;8(2):e0075.
6. **Han L**, **Liu H**, **Fu H**, **Hu Y**, **Fang W**, **Liu J**. Exosome-delivered BMP-2 and polyaspartic acid promotes tendon bone healing in rotator cuff tear via Smad/RUNX2 signaling pathway. *Bioengineered*. 2022;13(1):1459–1475.
7. **Ibounig T**, **Simons T**, **Launonen A**, **Paavola M**. Glenohumeral osteoarthritis: an overview of etiology and diagnostics. *Scand J Surg*. 2021;110(3):441–451.
8. **Coifman I**, **Brunner UH**, **Scheibel M**. Dislocation arthropathy of the shoulder. *J Clin Med*. 2022;11(7):2019.
9. **Gelberman RH**, **Menon J**, **Austerlitz MS**, **Weisman MH**. Pyogenic arthritis of the shoulder in adults. *J Bone Joint Surg Am*. 1980;62-A(4):550–553.
10. **Kaandorp CJ**, **Dinant HJ**, **van de Laar MA**, **Moens HJ**, **Prins AP**, **Dijkmans BA**. Incidence and sources of native and prosthetic joint infection: a community based prospective survey. *Ann Rheum Dis*. 1997;56(8):470–475.
11. **Voss A**, **Pfeifer CG**, **Kerschbaum M**, **Rupp M**, **Angele P**, **Alt V**. Postoperative septic arthritis after arthroscopy: modern diagnostic and therapeutic concepts. *Knee Surg Sports Traumatol Arthrosc*. 2021;29(10):3149–3158.
12. **Porcellini G**, **Merolla G**, **Campi F**, **Pellegrini A**, **Bodanki CS**, **Paladini P**. Arthroscopic treatment of early glenohumeral arthritis. *J Orthop Traumatol*. 2013;14(1):23–29.
13. **Kerr R**, **Resnick D**, **Pineda C**, **Haghighi P**. Osteoarthritis of the glenohumeral joint: a radiologic-pathologic study. *AJR Am J Roentgenol*. 1985;144(5):967–972.
14. **Matson AP**, **Kunkel Z**, **Bernal-Crespo VA**, **et al**. The histopathology of the humeral head in glenohumeral osteoarthritis. *Osteoarthr Cartil Open*. 2021;3(2):100147.

15. **Hsu H-C**, **Luo Z-P**, **Stone JJ**, **Huang T-H**, **An K-N**. Correlation between rotator cuff tear and glenohumeral degeneration. *Acta Orthop Scand*. 2003;74(1):89–94.
16. **Toma T**, **Suenaga N**, **Taniguchi N**, **et al**. Humeral head histopathological changes in cuff tear arthropathy. *J Orthop Surg (Hong Kong)*. 2019;27(1):230949901881642.
17. **Abrams GD**, **Luria A**, **Carr RA**, **Rhodes C**, **Robinson WH**, **Sokolove J**. Association of synovial inflammation and inflammatory mediators with glenohumeral rotator cuff pathology. *J Shoulder Elbow Surg*. 2016;25(6):989–997.
18. **Chainani A**, **Matson A**, **Chainani M**, **et al**. Contracture and transient receptor potential channel upregulation in the anterior glenohumeral joint capsule of patients with end-stage osteoarthritis. *J Shoulder Elbow Surg*. 2020;29(7):e253–e268.
19. **Toegel S**, **Bieder D**, **André S**, **et al**. Human osteoarthritic knee cartilage: fingerprinting of adhesion/growth-regulatory galectins in vitro and in situ indicates differential upregulation in severe degeneration. *Histochem Cell Biol*. 2014;142(4):373–388.
20. **Walzer SM**, **Toegel S**, **Chiari C**, **et al**. A 3-dimensional *in vitro* model of zonally organized extracellular matrix. *Cartilage*. 2021;13(2_suppl):336S–345S.
21. **Krenn V**, **Morawietz L**, **Häupl T**, **Neidel J**, **Petersen I**, **König A**. Grading of chronic synovitis--a histopathological grading system for molecular and diagnostic pathology. *Pathol Res Pract*. 2002;198(5):317–325.
22. **Pichler KM**, **Fischer A**, **Alphonsus J**, **et al**. Galectin network in osteoarthritis: galectin-4 programs a pathogenic signature of gene and effector expression in human chondrocytes in vitro. *Histochem Cell Biol*. 2022;157(2):139–151.
23. **Jayadev C**, **Rout R**, **Jackson W**, **Price A**, **Hulley P**. Synovial fluid preparation to improve immunoassay precision for biomarker research using multiplex platforms. *Osteoarthr Cartilage*. 2012;20:S84–S85.
24. **Ranstam J**. Repeated measurements, bilateral observations and pseudoreplicates, why does it matter? *Osteoarthr Cartil*. 2012;20(6):473–475.
25. **Fox JA**, **Cole BJ**, **Romeo AA**, **et al**. Articular cartilage thickness of the humeral head: an anatomic study. *Orthopedics*. 2008;31(3):216.
26. **Killian ML**, **Cavinatto L**, **Galatz LM**, **Thomopoulos S**. Recent advances in shoulder research. *Arthritis Res Ther*. 2012;14(3):214.
27. **Chubinskaya S**, **Cotter EJ**, **Frank RM**, **Hakimiyan AA**, **Yanke AB**, **Cole BJ**. Biologic characteristics of shoulder articular cartilage in comparison to knee and ankle articular cartilage from individual donors. *Cartilage*. 2021;12(4):456–467.
28. **Yuan G-H**, **Tanaka M**, **Masuko-Hongo K**, **et al**. Characterization of cells from pannus-like tissue over articular cartilage of advanced osteoarthritis. *Osteoarthr Cartilage*. 2004;12(1):38–45.
29. **Weinmann D**, **Schlangen K**, **André S**, **et al**. Galectin-3 induces a pro-degradative/inflammatory gene signature in human chondrocytes, teaming up with Galectin-1 in osteoarthritis pathogenesis. *Sci Rep*. 2016;6:39112.
30. **Allard SA**, **Muirden KD**, **Maini RN**. Correlation of histopathological features of pannus with patterns of damage in different joints in rheumatoid arthritis. *Ann Rheum Dis*. 1991;50(5):278–283.
31. **Hu Y**, **Chen X**, **Wang S**, **Jing Y**, **Su J**. Subchondral bone microenvironment in osteoarthritis and pain. *Bone Res*. 2021;9(1):20.
32. **Li G**, **Yin J**, **Gao J**, **et al**. Subchondral bone in osteoarthritis: insight into risk factors and microstructural changes. *Arthritis Res Ther*. 2013;15(6):223.
33. **Goldring MB**, **Otero M**, **Tsuchimochi K**, **Ijiri K**, **Li Y**. Defining the roles of inflammatory and anabolic cytokines in cartilage metabolism. *Ann Rheum Dis*. 2008;67 Suppl 3(0 3):iii75–82.
34. **Grogan SP**, **Miyaki S**, **Asahara H**, **D'Lima DD**, **Lotz MK**. Mesenchymal progenitor cell markers in human articular cartilage: normal distribution and changes in osteoarthritis. *Arthritis Res Ther*. 2009;11(3):R85.
35. **Toegel S**, **Weinmann D**, **André S**, **et al**. Galectin-1 couples glycobiology to inflammation in osteoarthritis through the activation of an NF-κB–regulated gene network. *J Immunol*. 2016;196(4):1910–1921.
36. **Weinmann D**, **Kenn M**, **Schmidt S**, **et al**. Galectin-8 induces functional disease markers in human osteoarthritis and cooperates with galectins-1 and -3. *Cell Mol Life Sci*. 2018;75(22):4187–4205.
37. **Pichler KM**, **Weinmann D**, **Schmidt S**, **et al**. The dysregulated galectin network activates NF-κB to induce disease markers and matrix degeneration in 3D pellet cultures of osteoarthritic chondrocytes. *Calcif Tissue Int*. 2021;108(3):377–390.
38. **Marcu KB**, **Otero M**, **Olivotto E**, **Borzi RM**, **Goldring MB**. NF-kappaB signaling: multiple angles to target OA. *Curr Drug Targets*. 2010;11(5):599–613.
39. **Noh K-C**, **Park S-H**, **Yang CJ**, **Lee GW**, **Kim MK**, **Kang Y-H**. Involvement of synovial matrix degradation and angiogenesis in oxidative stress-exposed degenerative rotator cuff tears with osteoarthritis. *J Shoulder Elbow Surg*. 2018;27(1):141–150.
40. **Jo CH**, **Shin JS**, **Kim JE**, **Oh S**. Macroscopic and microscopic assessments of the glenohumeral and subacromial synovitis in rotator cuff disease. *BMC Musculoskelet Disord*. 2015;16:272.
41. **Casagrande D**, **Stains JP**, **Murthi AM**. Identification of shoulder osteoarthritis biomarkers: comparison between shoulders with and without osteoarthritis. *J Shoulder Elbow Surg*. 2015;24(3):382–390.
42. **Horton WA**, **Dwyer C**, **Goering R**, **Dean DC**. Immunohistochemistry of types I and II collagen in undecalcified skeletal tissues. *J Histochem Cytochem*. 1983;31(3):417–425.
43. **Martin I**, **Jakob M**, **Schäfer D**, **Dick W**, **Spagnoli G**, **Heberer M**. Quantitative analysis of gene expression in human articular cartilage from normal and osteoarthritic joints. *Osteoarthr Cartilage*. 2001;9(2):112–118.
44. **Toegel S**, **Pabst M**, **Wu SQ**, **et al**. Phenotype-related differential α-2,6- or α-2,3-sialylation of glycoprotein N-glycans in human chondrocytes. *Osteoarthr Cartil*. 2010;18(2):240–248.
45. **Dejica VM**, **Mort JS**, **Laverty S**, **et al**. Increased type II collagen cleavage by cathepsin K and collagenase activities with aging and osteoarthritis in human articular cartilage. *Arthritis Res Ther*. 2012;14(3):R113.
46. **Olivotto E**, **Otero M**, **Astolfi A**, **et al**. IKKα/CHUK regulates extracellular matrix remodeling independent of its kinase activity to facilitate articular chondrocyte differentiation. *PLoS One*. 2013;8(9):e73024.
47. **Cui S**, **Li W**, **Teixeira GQ**, **et al**. Neoepitope fragments as biomarkers for different phenotypes of intervertebral disc degeneration. *JOR Spine*. 2022;5(3):e1215.
48. **Eltawil NM**, **De Bari C**, **Achan P**, **Pitzalis C**, **Dell'Accio F**. A novel in vivo murine model of cartilage regeneration. Age and strain-dependent outcome after joint surface injury. *Osteoarthr Cartilage*. 2009;17(6):695–704.
49. **Hawellek T**, **Hubert J**, **Hischke S**, **et al**. Articular cartilage calcification of the humeral head is highly prevalent and associated with osteoarthritis in the general population. *J Orthop Res*. 2016;34(11):1984–1990.
50. **Kim D-H**, **Bae K-C**, **Choi J-H**, **Na S-S**, **Hwang I**, **Cho C-H**. Chronicity is associated with the glenohumeral synovitis in patients with a rotator cuff tear. *J Orthop Res*. 2021;39(10):2226–2233.
51. **Shindle MK**, **Chen CCT**, **Robertson C**, **et al**. Full-thickness supraspinatus tears are associated with more synovial inflammation and tissue degeneration than partial-thickness tears. *J Shoulder Elbow Surg*. 2011;20(6):917–927.
52. **Thomas NP**, **Wu WJ**, **Fleming BC**, **Wei F**, **Chen Q**, **Wei L**. Synovial inflammation plays a greater role in post-traumatic osteoarthritis compared to idiopathic osteoarthritis in the Hartley guinea pig knee. *BMC Musculoskelet Disord*. 2017;18(1):556.
53. **Schett G**, **Tohidast-Akrad M**, **Steiner G**, **Smolen J**. The stressed synovium. *Arthritis Res*. 2001;3(2):80–86.
54. **Landi A**, **Marotta N**, **Morselli C**, **Marongiu A**, **Delfini R**. Pannus regression after posterior decompression and occipito-cervical fixation in occipito-atlanto-axial instability due to rheumatoid arthritis: case report and literature review. *Clin Neurol Neurosurg*. 2013;115(2):111–116.
55. **Oka Y**, **Murata K**, **Kano T**, **et al**. Impact of controlling abnormal joint movement on the effectiveness of subsequent exercise intervention in mouse models of early knee osteoarthritis. *Cartilage*. 2021;13(2_suppl):1334S–1344S.
56. **Kanbe K**, **Takemura T**, **Takeuchi K**, **Chen Q**, **Takagishi K**, **Inoue K**. Synovectomy reduces stromal-cell-derived factor-1 (SDF-1) which is involved in the destruction of cartilage in osteoarthritis and rheumatoid arthritis. *J Bone Joint Surg Br*. 2004;86-B(2):296–300.

Author information

S. Toegel, MPharmS, PhD, Principal Investigator,
Department of Orthopedics and Trauma Surgery, Karl Chiari Lab for Orthopaedic Biology, Medical University of Vienna, Vienna, Austria;
Ludwig Boltzmann Institute for Arthritis and Rehabilitation, Vienna, Austria.

L. Martelanz, Scientific Assistant
J. Alphonsus, MD, PhD Student, Clinical Researcher
R. Gruebl-Barabas, Biomedical Analyst
M. Cezanne, Biomedical Analyst
M. Rothbauer, MSc, PhD, Group Leader
R. Windhager, MD, Head of Department
Department of Orthopedics and Trauma Surgery, Karl Chiari Lab for Orthopaedic Biology, Medical University of Vienna, Vienna, Austria.

L. Hirtler, Mag. DDr., Deputy Head of the Division of Anatomy, Division of Anatomy, Center for Anatomy and Cell Biology, Medical University of Vienna, Vienna, Austria.

P. Heuberer, MD, PhD, Clinical Researcher, healthPi, Vienna, Austria.

L. Pauzenberger, MD, PhD, Clinical Researcher, healthPi, Vienna, Austria; Orthopaedic Department, Evangelisches Krankenhaus Wien, Vienna, Austria.

Author contributions

S. Toegel: Conceptualization, Data curation, Formal analysis, Funding acquisition, Investigation, Methodology, Project administration, Resources, Validation, Visualization, Writing – original draft.
L. Martelanz: Data curation, Investigation, Methodology, Writing – review & editing.
J. Alphonsus: Investigation, Methodology, Writing – review & editing.
L. Hirtler: Resources, Writing – review & editing.
R. Gruebl-Barabas: Methodology, Writing – review & editing.
M. Cezanne: Methodology, Writing – review & editing.
M. Rothbauer: Formal analysis, Writing – review & editing.
P. Heuberer: Conceptualization, Project administration, Resources, Writing – review & editing.
R. Windhager: Resources, Supervision, Writing – review & editing.
L. Pauzenberger: Conceptualization, Project administration, Resources, Writing – review & editing.

Funding statement

The authors received no financial or material support for the research, authorship, and/or publication of this article.

Data sharing

The data that support the findings for this study are available to other researchers from the corresponding author upon reasonable request.

Acknowledgements

The authors thank the body donors and their families; without their support, this study would not have been possible. Alexander Stoegner, Bettina Rodriguez-Molina, and Cornelia Brunner are acknowledged for providing technical support.

Ethical review statement

The study was approved by the ethics committees of the Medical University of Vienna (EK-No.: 1727/2015) and St. Vincent Hospital Vienna (EK-No.: 201506_EK16).

Open access funding

The authors report that the open access funding for their manuscript was self-funded.